Masure, H. R., Shattuck, R. L., & Storm, D. R. (1988) *Microbiol. Rev. 51*, 60-65.
Miller, J. H. (1972) *Experiments in Molecular Genetics*, Cold Spring Harbor Laboratory, Cold Spring Harbor, NY.
Pai, E. R., Sachsenheimer, Schirmer, R. H., & Schulz, G. E. (1977) *J. Mol. Biol. 114*, 37-45.
Roberts, D. M., Crea, R., Melecha, M., Alvarado-Urbina, G., Chiarello, R. H., & Watterson, D. M. (1985) *Biochemistry 24*, 5090-5098.
Salomon, Y., Londos, D., & Rodbell, M. (1974) *Anal. Biochem. 58*, 541-548.
Sanger, F., Nicklen, S., & Coulson, A. R. (1977) *Proc. Natl. Acad. Sci. U.S.A. 74*, 5463-5467.
Shattuck, R. L., & Storm, D. R. (1985) *Biochemistry 24*, 6323-6328.
Silhavy, T. J., Berman, M. L., & Enquist, L. W. (1984) *Experiments with Gene Fusions*, Cold Spring Harbor Laboratory, Cold Spring Harbor, NY.
Wardlaw, A. C., & Parton, R. (1988) *Pathogenesis and Immunity in Pertussis*, Wiley, New York, NY.
Weiss, A. A., & Falkow, S. (1984) *Infect. Immun. 43*, 263-269.
Weiss, A. A., Hewlett, E. L., Myers, G. A., & Falkow, S. (1984) *J. Infect. Dis. 150*, 219-222.
Westcott, K. R., Olwin, B. B., & Storm, D. R. (1980) *J. Biol. Chem. 255*, 8767-8771.
Wolff, J., Cook, H., Goldhammer, A. R., & Berkowitz, S. A. (1980) *Proc. Natl. Acad. Sci. U.S.A. 77*, 3840-3844.
Young, R. A., & Davis, R. W. (1983) *Proc. Natl. Acad. Sci. U.S.A. 80*, 1194-1198.

Articles

Photoreceptor Channel Activation by Nucleotide Derivatives†

Jacqueline C. Tanaka,*,‡ John F. Eccleston,§ and Roy E. Furman‖
Department of Biochemistry and Biophysics and Department of Neurology, School of Medicine, University of Pennsylvania, Philadelphia, Pennsylvania 19104, and National Institute for Medical Research, Mill Hill, London NW7 1AA, U.K.
Received July 28, 1988; Revised Manuscript Received November 4, 1988

ABSTRACT: Cyclic nucleotide activated sodium currents were recorded from photoreceptor outer segment membrane patches. The concentration of cGMP and structurally similar nucleotide derivatives was varied at the cytoplasmic membrane face; currents were generated at each concentration by the application of a voltage ramp. Nucleotide-activated currents were analyzed as a function of both concentration and membrane potential. For cGMP, the average $K_{0.5}$ at 0 mV was 24 μM, and the activation was cooperative with an average Hill coefficient of 2.3. Of the nucleotide derivatives examined, only 8-[[(fluorescein-5-ylcarbamoyl)methyl]thio]-cGMP (8-Fl-cGMP) activated the channel at lower concentrations than cGMP with a $K_{0.5}$ of 0.85 μM. The next most active derivative was 2-amino-6-mercaptopurine riboside 3',5'-monophosphate (6-SH-cGMP) which had a $K_{0.5}$ of 81 μM. cIMP and cAMP had very high $K_{0.5}$ values of $\sim$1.2 mM and >1.5 mM, respectively. All nucleotides displayed cooperativity in their response and were rapidly reversible. Maximal current for each derivative was compared to the current produced at 200 μM cGMP; only 8-Fl-cGMP produced an identical current. The partial agonists 6-SH-cGMP, cIMP, and cAMP activated currents which were $\sim$90%, 80%, and 25% of the cGMP response, respectively. 5'-GMP, 2-aminopurine riboside 3',5'-monophosphate, and 2'-deoxy-cGMP produced no detectable current. The $K_{0.5}$ values for cGMP activation, examined from -90 to +90 mV, displayed a weak voltage dependence of $\sim$400 mV/*e*-fold; the index of cooperativity was independent of the applied field. The current-voltage relationship at saturating cGMP concentrations was fitted by a simple voltage-dependent closed to open conformational change. The voltage dependence of this conformational change did not, however, account entirely for the voltage-dependent shift in $K_{0.5}$. Similarly, the voltage dependence could not be explained by a charged ligand moving into a binding site within the membrane field.

In vertebrate photoreceptor outer segments, light energy absorbed by rhodopsin regulates the flow of an electrical current through a cation channel in the plasmalemma. The cell's response to light results in a decrease of 3',5'-cGMP, which closes the channel and reduces the transmembrane current. For the photoreceptor channel, cGMP is a rapidly reversible, direct agonist of channel gating with a $K_{0.5}$[1] from

† This work was supported by NIH Grants EY-06640, BRSG 07083-21, and 05415-25 to J.C.T., University Research Fund and NIH Grants NS 00865 and BRSG S07-RR-05415-26 to R.E.F., NIH Grant GM 25256 to Paul Mueller, and the U.K. Medical Research Council (J.F.E.).
* Address correspondence to this author at the Department of Biochemistry and Biophysics, University of Pennsylvania, 317 Anatomy Chemistry, 36 St. and Hamilton Walk, Philadelphia, PA 19104.
‡ Department of Biochemistry and Biophysics, University of Pennsylvania.
§ National Institute for Medical Research.
‖ Department of Neurology, University of Pennsylvania.

[1] Abbreviations: 8-Br-cGMP, 8-bromoguanosine 3',5'-monophosphate; 8-Fl-cGMP, 8-[[(fluorescein-5-ylcarbamoyl)methyl]thio]-guanosine 3',5'-monophosphate; 6-SH-cGMP, 2-amino-6-mercaptopurine riboside 3',5'-monophosphate; 2-amino-cPMP, 2-aminopurine riboside 3',5'-monophosphate; *I*, transmembrane current; I_{max}, current produced by saturating ligand concentrations; *V*, transmembrane potential; V_0, potential for an *e*-fold change; N_h, Hill index of cooperativity; $K_{0.5}$, ligand concentration for half-maximal current activation; K_o, apparent equilibrium dissociation constant for channel opening; K_b, apparent equilibrium dissociation constant for ligand binding; *L*, ligand concentration, *IV*, plot of membrane current versus membrane voltage.

0006-2960/89/0428-2776$01.50/0

12 to 40 μM [see reviews by Pugh and Cobbs (1986) and Yau et al. (1986)] and a Hill coefficient from 1.6 to 3.4, indicating as many as four nucleotides may be required to open each channel. The photoreceptor channel is the best characterized example of a class of nucleotide-gated, sensory transduction ion channels which, so far, include the olfactory cilia channels (Nakamura & Gold, 1987) and taste receptor channels (Tonosaki & Funakoshi, 1988).

Ion channels are specialized, high-turnover enzymes ($>10^5$–10^6 molecules/s) that, besides being dependent on the classical state parameters of substrate concentration, temperature, pH, cofactors, activators, etc., depend on a thermodynamic state function, transmembrane potential. Our interest in this paper is the molecular mechanism of cGMP-activated channel gating viewed from the traditional perspective of structure–activity relations of nucleotide activators and cooperative ligand binding interactions (Hill, 1910; Adair, 1925; Weber & Anderson, 1965) and from the physiological perspective of voltage-dependent channel reaction mechanisms.

To characterize the structure–activity relations of nucleotide binding, we have measured the dose–response relation for a series of purine-substituted cGMP derivatives which had changes in the C(2), C(6), or C(8) positions on the purine ring or the 3′,5′-diester and 2′-oxygen on the ribose. Analysis of structure–activity relations for nucleotide activators shows that the cGMP-activated channel binding sites share functional similarities with the nucleotide binding sites from elongation factor Tu, in which the sequence (Arai et al., 1980) and the structure of the binding domain have been described (Jurnak, 1985; La Cour et al., 1985), and on the catabolite gene activation protein, in which the crystal structure is known (Weber et al., 1982). Additionally, we have found several partial agonists of the photoreceptor channel and a potentially physiologically important modulator of cGMP activation, cAMP, whose properties are detailed in the companion paper (Furman & Tanaka, 1989).

Membrane potential may influence channel function by its effect on substrate concentration, activator concentration, or the dipole moments of the channel protein's structure. By examining the voltage dependence of the channel reaction and assigning the voltage dependence to one or more steps of the reaction, we can develop or constrain models of the reaction mechanism. This approach has been exploited in studies of voltage- and ligand-activated ion channels to localize gating regions of the protein, ion binding and blocking sites in the permeation pathway, and toxin or ligand binding sites [see Hille (1985)]. Such predictions have become central to the construction of the channel topology from the primary protein sequences of cloned ion channels [see review by Catterall (1988)].

To distinguish direct binding responses from subsequent activation of the ion channel pathway, we fitted the *IV* relation at saturating concentrations of nucleotide with a simple two-state, voltage-dependent open–close model. Dose–response relations for each nucleotide were then fitted with a linear, sequential, binding-activation model which allowed us to infer the voltage dependence of binding separately from the voltage dependence of channel activation. Contrary to expectations and previous reports (Karpen et al., 1988), we found that neither the charge on the activating ligand nor the voltage dependence of channel gating accounts for all the apparent voltage dependence of binding.

Materials and Methods

Materials. cGMP was obtained from Sigma, Chemical Dynamics Corp., and Calbiochem. cAMP and 2′-deoxy-cGMP were obtained from Sigma and Boehringer Mannheim. cIMP, 6-thioguanosine, and GMP were obtained from Sigma, and 5-(iodoacetamido)fluorescein was from Molecular Probes.

Several species of amphibians, including both Northern and Southern *Rana pipiens* and *Bufo marinus*, were used for excised patch experiments; no systematic differences in the cGMP-activated currents were found among the species.

Preparation of cGMP Analogues. 8-Fl-cGMP was prepared by a method similar to the method of Caretta et al. (1985). We were unable, however, to convert 8-Br-cGMP to 8-SH-cGMP by reaction with thiourea at room temperature. Heating the reaction mixture under reflux for 12 h was necessary for the formation of the product. The 8-SH-cGMP was purified by DEAE-cellulose (DE52) column chromatography using a triethylammonium bicarbonate gradient (0–0.4 M) before reaction with 5-(iodoacetamido)fluorescein. The product was purified in a similar way but with a 0–1 M gradient. Its behavior on TLC and its absorption spectrum were identical with those reported by Caretta et al. (1985).

6-SH-cGMP was prepared by phosphorylation of 6-thioguanosine with $POCl_3$ according to the method described for the synthesis of formycin 5′-monophosphate by Rossomando et al. (1981). 2-Amino-PMP was prepared by desulfurization of 6-SH-GMP with Raney nickel as described for the nucleoside by Fox et al. (1958). The 5′-phosphate group remained intact during this procedure, and the 2-amino-PMP was purified on a DEAE-cellulose column in the bicarbonate form, elution being with a gradient of 0–0.3 M triethylammonium bicarbonate. 6-Thio-GMP and 2-amino-PMP were both converted to the 3′,5′-cyclic derivatives by the procedure of Smith et al. (1961) using the 4-morpholino-*N*,*N*′-dicyclohexylcarboxamidium salt of the nucleotides. They were purified as described for 2-amino-PMP.

^{31}P NMR spectra of all the cyclic nucleotides synthesized showed a doublet with approximately 20-Hz splitting which collapsed to a single peak on proton decoupling. These results are consistent with the six-membered phosphate ring in the nucleotides since the coupling constants of 3′H, 5′H, and 5″H to phosphate in cGMP are 2.1, 1.9, and 21.6 Hz, respectively (Lee & Sarma, 1976).

Progress of synthetic reactions and purity of the cyclic nucleotides were determined by analysis on HPLC (Waters C-18 μBondapak column eluted with 10 mM KH_2PO_4, pH 5.5, and 10% methanol at 1.5 mL/min). The nucleotide structures are shown in Figure 1.

Patch Recordings. The retinas of dark-adapted animals were dissected under red light and maintained in cold frog Ringer's solution containing 120 mM NaCl, 10 mM HEPES, pH 7.4, 1 mM $CaCl_2$, 1 mM $MgCl_2$, and 0.05 mM EGTA. The experimental solutions used in both the patch electrodes and bath contained 120 mM NaCl, 5 mM HEPES, pH 7.4, and 2 mM EGTA (Na) (solution A). Free calcium in solution A, measured with a calcium-selective electrode, was less than instrumental resolution ($<10^{-7}$ M). Free magnesium levels were assumed to be less than free calcium due to the significantly higher affinity of EGTA for Mg^{2+}.

Photoreceptors were layered onto the floor of the experimental chamber, and currents were recorded from excised inside-out patches as previously described (Furman & Tanaka, 1988) with Corning 0010 glass micropipets which had been washed first in chloroform–methanol (2:1) and then rinsed in distilled water. All experiments were done in room light at 19–22 °C. The patch clamp amplifier output (Dagan 8900) was low-pass filtered at 1 kHz (8-pole Bessel) before display on an oscilloscope and digitization by an IBM AT (5 kHz,

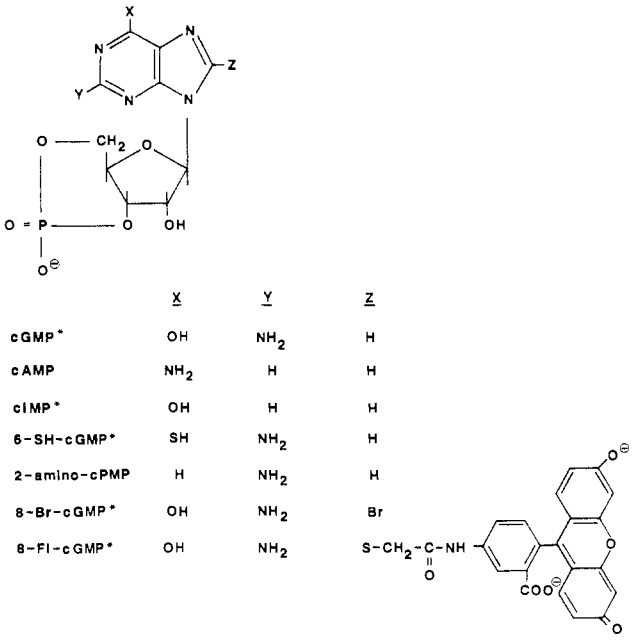

	X	Y	Z
cGMP*	OH	NH_2	H
cAMP	NH_2	H	H
cIMP*	OH	H	H
6-SH-cGMP*	SH	NH_2	H
2-amino-cPMP	H	NH_2	H
8-Br-cGMP*	OH	NH_2	Br
8-Fl-cGMP*	OH	NH_2	$S-CH_2-C-NH$

FIGURE 1: Chemical structures of cGMP analogues. The compounds indicated with an asterisk exist as keto (thione) structures so that the proton in 6-OH is actually on N-1.

12-bit A/D). Current–voltage relations were measured by stimulating the patch with a linear voltage ramp (260 mV/s) from −90 to +90 mV and back to −90 mV. Digitized currents from the up and down ramp were averaged to compensate for linear capacitative currents produced by the ramp [see Furman and Tanaka (1988)]. This protocol was used for dose–response measurements to permit rapid data acquisition and to minimize destabilization of the patch which often occurred after a series of 50-ms voltage steps. In all figures the small, linear leakage current measured without cGMP (typically <0.2–0.5% of the maximal cGMP-activated current) was digitally subtracted from the total current measured in the test solution. Currents, potentials, and membrane surfaces are reported in physiological conventions.

After an inside-out patch was formed, the pipet tip was positioned in the stream of the inflow tube which was fed by 1 of 12 solutions manually selected with a rotary valve. Equilibration with a new concentration of nucleotide usually occurred within 30 s after a solution switch, and currents were recorded 1 min after the solution was switched. All patches were tested for activity with a saturating concentration of cGMP (200 μM) at the beginning and conclusion of a series of analogue test solutions. Generally, concentration–response experiments were determined at 8–10 concentrations.

In control experiments, no differences were seen in the *IV* curves produced by the voltage ramp and by a series of 100-ms voltage steps (Furman and Tanaka, unpublished results). We have therefore concluded that the concentration responses to the applied voltage ramp represent steady-state current measurements.

Data Analysis. The *IV* relations at each ligand concentration were converted by computer to current–ligand concentration curves as a function of voltage. Experimental dose–response data were analyzed at 10-mV intervals by fitting the data directly to the Hill equation

$$I = I_{max}/[1 + (K_{0.5}/L)^{N_h}] \quad (1)$$

with a Levenberg–Marquardt algorithm for nonlinear, weighted, least-squares fitting (Press et al., 1986), where I is the measured current and L is the concentration of the applied nucleotide. Initial estimates were made for the parameters I_{max} (the current at saturation with ligand), $K_{0.5}$ (the ligand concentration at half-saturation), and N_h (the index of cooperativity). The goodness of fit of the data to the model was estimated by calculating the incomplete γ function Q for the probability that a value of χ^2 as poor as the observed value should occur by chance. A fit was deemed acceptable for $Q > 0.01$. Other reaction schemes described in the text were also fit to the data with analogous procedures.

RESULTS

cGMP Activation of Membrane Current. cGMP directly activates a cationic membrane channel in excised, inside-out patches pulled from the outer segments of rods as was first shown by Fesenko et al. (1985). Under physiological conditions, the current activated by cGMP shows strong outward rectification, i.e., the current increases steeply with depolarization, but with hyperpolarization, the current is small and nearly constant. This rectification has been attributed to a voltage-dependent block of the channel by divalent cations [see review by Yau et al. (1986)]. Replacing physiological solutions with symmetrical, divalent-free 120 mM NaCl solutions significantly increases the current magnitude and reduces the degree of outward rectification. These conditions were chosen, therefore, to minimize divalent block of the currents and possible divalent interactions with nucleotide activation.

As the cGMP concentration perfusing the cytoplasmic face of the patch increases from 1 to 300 μM, the absolute magnitudes of the current increase, but the current–voltage (*IV*) curves remain qualitatively similar (Figure 2A). The current magnitudes varied widely from patch to patch but, on average, were ~1 nA at saturating concentrations of cGMP, similar to those previously recorded without divalent cations (Haynes et al., 1986; Zimmerman & Baylor, 1986; Furman & Tanaka, 1988).

Activation by cGMP Analogues. 8-Fl-cGMP, 6-SH-cGMP, cIMP, and cAMP produced responses qualitatively similar to those seen with cGMP. Currents showed saturation with increasing nucleotide concentration, were rapidly reversible following removal of the nucleotide, and had a sigmoidal dose–response relation implying several nucleotide molecules were necessary to activate fully each channel. The shape of the *IV* responses of the analogues was similar to that of the response for cGMP shown in Figure 2A. The major differences between the derivatives and cGMP were the $K_{0.5}$ values and I_{max}, the maximal current activated at saturating nucleotide concentrations (Table I).

8-Fl-cGMP was the only analogue with a lower $K_{0.5}$ than cGMP (0.85 μM, Table I), and the maximal 8-Fl-cGMP-activated current was indistinguishable from the current activated by saturating cGMP. The average Hill coefficient for 8-Fl-cGMP was 1.7 compared with 2.3 for cGMP (Table I). We have not interpreted these values as significantly different, however, due to the large variation in the steepness of the dose–response relation from patch to patch, and because of the slow solution exchange time, it was not possible to compare full concentration–response curves for two nucleotides on a single patch before the seal deteriorated.

The reference compound, cGMP, has a 2-amino group and a 6-oxy group on the purine ring (Figure 1). Substituting a sulfhydryl group at the 6-position produced a slightly less effective analogue, 6-SH-cGMP, which had a $K_{0.5}$ of 81 μM, about 3-fold higher than the $K_{0.5}$ for cGMP. The current activated at saturating concentrations of 6-SH-cGMP was ~90% of the maximal cGMP current, and the average index of cooperativity, N_h, was 2.6.

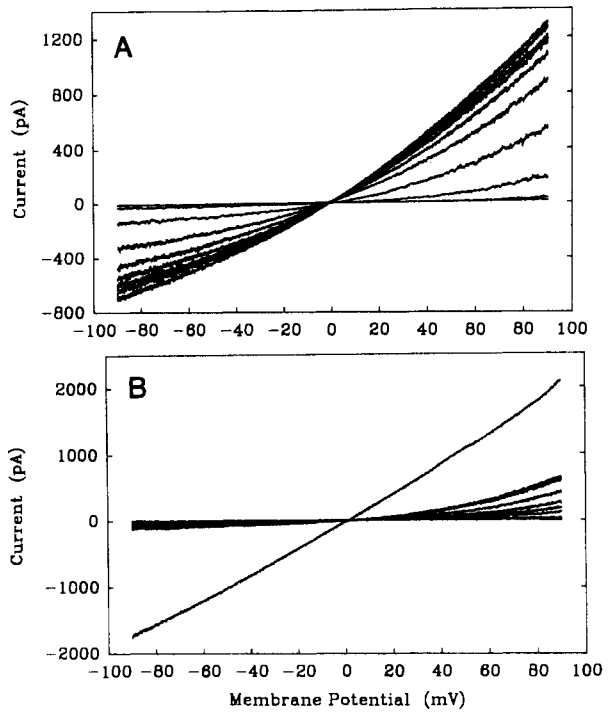

FIGURE 2: Nucleotide-dependent current activation in an excised inside/out patch from an outer segment membrane. (A) cGMP-activated currents were collected during a 750-ms voltage ramp from −90 to +90 mV. The currents increased as [cGMP] was increased at 1, 2, 5, 10, 20, 30, 50, 80, 100, and 300 μM. The reversal potential for the currents was 0 mV as expected with identical bath and pipet solutions. The outward (positive) currents increased at lower concentrations than the inward currents and were ~2-fold greater at saturating concentrations of cGMP (patch 75271). (B) The patch was perfused with cAMP alone at 0.1, 0.25, 0.5, 0.8, 1.0, 2.0, 5.0, 7.5, and 10 mM concentrations. The current activated by 200 μM cGMP is the large, single trace. Following this series, the cGMP current was again measured and remained unchanged from the initial response. The cAMP currents show saturation, although the saturating value at +90 mV is ~20% of the cGMP-activated current. The concentration–response function for this patch is shown in Figure 3 (patch 81211).

Table I: Comparison of the Activation Properties of cGMP Analogues[a]

derivative [(n)]	$K_{0.5}$ ± SEM	K_b ± SEM (μM)	N_h ± SEM	current (%) in	current (%) out
8-Fl-cGMP (4)	0.85 ± 0.23 μM	1.14 ± 0.44	1.7 ± 0.3	100	100
cGMP (5)	24.1 ± 8.8 μM	26.8 ± 8.9	2.3 ± 0.5	100	100
6-SH-cGMP (2)	81.0 ± 27.0 μM	147 ± 1.4	2.6 ± 0.1	95	88
cIMP (2)	1150 μM	1690	3.4 ± 0.3	78	78
cAMP (4)	1502 ± 308 μM		1.4 ± 0.4	12	25
8-Br-cGMP	1.6 μM[b]				
2-amino-cPMP (3)	>2–5 mM[c]			0	0
GMP	>10 mM[c]			0	0
2′-deoxy-cGMP	>10 mM[c]			0	0

[a] The $K_{0.5}$ and N_h values are expressed as the means ± standard error of the mean (SEM), extrapolated to 0 mV for all patches tested. Inward and outward current values represent the fraction of current, activated at saturating concentrations of the derivative, compared with the current activated with 200 μM cGMP. Currents were measured at ±80 mV. [b] Results for 8-Br-cGMP were taken from Zimmerman et al. (1985). [c] These values were estimated by assuming the test nucleotide would activate 20% of a 200-pA maximal current with a small (<2 pA) leak current.

Removing the 2-amino group of cGMP yields cIMP which activated the channel only at high concentrations with a $K_{0.5}$ of ~1.2 mM. The average cooperativity was 3.4 for the two patches for which the entire range of nucleotides was measured. cIMP was also a partial agonist producing only ~80% of the cGMP-activated current.

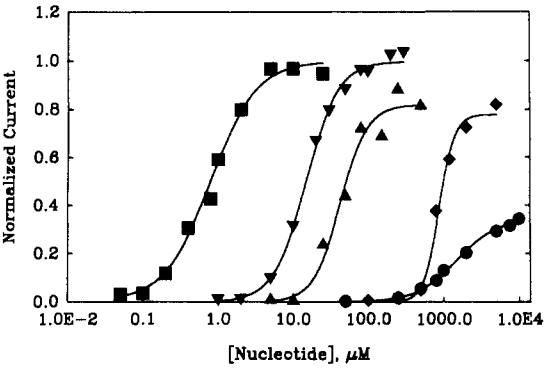

FIGURE 3: Normalized concentration–response relations for cGMP analogues in representative patches. The currents activated by nucleotide analogues were scaled by the current activated with 200 μM cGMP in the same patch. Data were fit with eq 1 (solid line). The average current and best fit are shown at +80 mV for 8-Fl-cGMP (■), cGMP (▼), 6-SH-cGMP (▲), cIMP (◆), and cAMP (●). $K_{0.5}$ values for the derivatives span more than 3 log units. Differences in the cooperativity are apparent from the steepness of the slopes. While some of this variation may reflect differences in the nucleotide, we saw large variability in the cooperativity from patch to patch (see text). Average $K_{0.5}$ and N_h values are presented in Table I for each derivative.

Substituting a 6-amino group for the 6-oxy group on cIMP yields cAMP, the weakest partial agonist studied. cAMP was effective in activating small currents at high concentrations (>2 mM) in all patches tested ($n > 20$). The most interesting feature of cAMP activation was the small fraction of maximal current activated at saturating concentrations of nucleotide, shown in Figure 2B. At saturation, the cAMP-activated current is less than ~25% of the maximal cGMP-activated current. The mean $K_{0.5}$ was ~1.5 mM with a cooperativity index of 1.4 (Table I).

To rule out the possibility that cAMP and cIMP, which had very high $K_{0.5}$ values, contained sufficient cGMP contamination to account for their activity, we analyzed the stock solutions on HPLC as described under Materials and Methods. No cGMP could be detected in the cAMP or cIMP samples, suggesting <0.02% contamination. Further evidence for a specific cAMP effect is seen with experiments mixing cGMP and cAMP (Furman & Tanaka, 1989).

The normalized concentration–response data for all active derivatives are summarized in Figure 3 and Table I. The relative efficacy is 8-Fl-cGMP > cGMP > 6-SH-cGMP ≫ cIMP ~ cAMP. A comparison of the maximal currents shows cGMP = 8-Fl-cGMP > 6-SH-cGMP > cIMP ≫ cAMP.

Inactive Derivatives. 5′-GMP (1 mM), 2′-deoxy-cGMP (200 μM), and 2-amino-cPMP (200 μM) produced no detectable current. These derivatives were also tested in the presence of 40 μM cGMP for their ability to modify the cGMP-activated current. Any change in the cGMP current would suggest that the derivative could bind, but not activate, the channel. None of these derivatives affected the cGMP response, and therefore, we conclude that they do not bind to the channel.

Structural Requirements for Channel Activation. Our observations have extended the number of structural analogues of cGMP (Figure 1) known to activate photoreceptor channels. 8-Fl-cGMP activated currents in a cooperative manner at much lower concentrations as reported originally by Caretta et al. (1985). Three partial agonists, 6-SH-cGMP, cIMP, and

cAMP showed significant differences only in the maximal current and apparent concentrations for half-maximal activation. Previous reports which showed no activation by cAMP (Fesenko et al., 1985; Haynes & Yau, 1985; Cobbs et al., 1985) are perhaps not surprising if we consider the small currents expected at subsaturating concentrations of cAMP. For example, at 1 mM, which is close to the $K_{0.5}$, one would expect ~10% of the maximal cGMP current.

The effect of these cGMP analogues on macroscopic currents in photoreceptor outer segment membranes allows us to derive information about the nucleotide binding site(s) of the channel. The presence of the six-membered cyclic phosphate ring is obviously essential for binding since 5′-GMP is neither an agonist nor an antagonist. Presumably, the single negative charge of the phosphodiester interacts with a positively charged amino acid residue of the channel as occurs in the interaction of cAMP with arginine 82 of catabolite gene activation protein (Weber et al., 1982). Zimmerman et al. (1985) have shown that both the *pro-S* and *pro-R* oxygen atoms of the phosphodiester are necessary for channel opening.

The 6-oxy and 2-amino groups of the purine ring play an important part in ligand interaction with the binding site, although some modification can be made while retaining detectable binding. Omission of the 2-amino group (cIMP and cAMP) or replacement of the 6-oxy group by 6-thio (6-SH-cGMP) reduces the affinity of the nucleotide for the channel whereas omission of the 6-oxy group (2-amino-cPMP) results in the complete abolishment of binding. These effects are similar to those observed in the binding of guanine nucleotide analogues to elongation factor Tu (Wittinghofer et al., 1977; Eccleston, 1981), where both the sequence (Arai et al., 1980) and the structure of its nucleotide binding domain have been described (Jurnak, 1985; La Cour et al., 1985). In this protein–GDP complex, O(6) forms a hydrogen bond with asparagine 135 while aspartate 138 forms hydrogen bonds to N(1) and/or N(2) of guanine.

The effects of nucleotide analogues differ markedly between the channel and elongation factor Tu when the 8-position is modified. Modification of the 8-position with bromine (Zimmerman et al., 1985) increases the binding affinity of the channel for nucleotide over that for cGMP, whereas the same modification to GDP reduces its affinity to elongation factor Tu (Wittinghofer et al., 1977). Introduction of an 8-[[(fluorescein-5-ylcarbamoyl)methyl]thio] moiety increases the binding of cGMP to the channel even more than the 8-Br group; data on an equivalent modification in the elongation factor Tu system are not available. The simplest explanation for this effect is substitution at the 8-position of cGMP results in formation of the syn conformation of the nucleotide, and this may be the form bound by the channel whereas elongation factor Tu binds GDP in the anti form (Jurnak, 1985). The predicted structures of the cAMP binding domains of cAMP-dependent protein kinase are consistent with the cAMP being bound in the syn form (Weber et al., 1987) although the crystal structure of catabolite gene activation protein shows cAMP to be in the anti form (Weber et al., 1982).

The structure of the elongation factor Tu–GDP complex shows that the 2′,3′-*cis*-diol of GDP projects out of the protein into the solvent (Jurnak, 1985; La Cour et al., 1985), a result confirmed by solution studies in which large fluorophores can be introduced at this position without significantly affecting binding (Eccleston et al., 1987). In contrast, the 2′-OH group of cAMP is essential for binding to catabolite gene activation protein (Ebright et al., 1985). This position is also critical for the cGMP-activated channel as 2′-deoxy-cGMP possessed neither agonist nor antagonist activity.

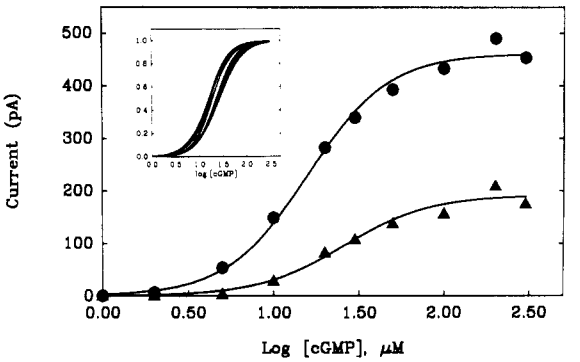

FIGURE 4: Voltage dependence of the concentration–response relation for cGMP-activated currents at two potentials. A family of cGMP-activated currents, similar to those of Figure 2A, were digitally averaged at +90 ± 0.5 mV (●) and −90 mV (▲) at each concentration of cGMP, and the best fit to the Hill equation (eq 1) was determined (solid line). Inward currents were smaller with I_{max} = 189 pA at −90 mV and 460 pA at 90 mV; the $K_{0.5}$'s were 26 and 16 μM, respectively. This concentration–response shows a cooperative index of 1.8 for N_h. For all measurements, standard deviations of the currents were smaller than the symbols (patch 75284). (Inset) Maximal currents at each 10-mV interval were scaled by the current at 90 mV and fitted to the Hill equation (eq 1); the ordinate is normalized current. Potentials from −20 to +20 mV, which had very small currents, were omitted. Traces shift from left to right as the potential decreases from +90 mV. The apparent affinity of cGMP for the channel increases with depolarization, but the index of cooperativity (slope at 0.5) is unaffected (patch 75284).

The $K_{0.5}$ values from steady-state macroscopic concentration–current curves reflect the ligand association steps and channel conformational change(s) from the closed to open state (see below). The original motivation for using a fluorescein-labeled high-affinity derivative was to measure steady-state fluorescence polarization to detect nucleotide binding in an attempt to separate the energetics of ligand binding from the entire reaction scheme. The polarization, however, did not increase sufficiently in our membrane preparations to provide a reliable measure of the binding. Since both 8-substituted derivatives appear to bind more tightly than cGMP, attaching other reporter groups at this location holds promise for future derivatives.

Partial Agonists. A comparison of 8-Fl-cGMP activation to that of cGMP shows no difference in the maximal currents; the simplest, though not the only, interpretation is that the number of channels, the single channel conductance, and the gating probability are unchanged and only the ligand binding kinetics are altered. The situation is more complex with the other derivatives, however, because the currents are attenuated, suggesting one or more of these parameters are changed. As shown in the following paper (Furman & Tanaka, 1989), the cGMP and cAMP competition experiments are not consistent with the existence of separate channel populations, and we conclude that either the individual channel conductance or the probability of opening is altered.

Voltage Dependence of Nucleotide Activation. The relation between cGMP concentration and current activation is shown in Figure 4 for two potentials, ±90 mV, at the extremes of the applied voltage. The saturating current, I_{max}, is greater, and the nucleotide concentration at half-saturation, $K_{0.5}$, is less, with depolarization than with hyperpolarization. The solid lines represent the best fit of an empirical relation, the Hill equation (eq 1), to the data. In this patch the ratio of outward/inward current at saturation was 2.4, and $K_{0.5}$ decreased by 1.6 from −90 to +90 mV. The slope, or index of cooperativity, of the two curves as measured by the Hill parameter,

Table II: Comparison of the Voltage Dependence of Photoreceptor Channel Activation among cGMP Analogues[a]

		Hill	receptor effector		
derivative [(n)]	charge	$K_{0.5}(V)$ (μM)	$K_b(V)$ (μM)	$K_o(0)$	V_0 (mV)
Fl-cGMP (4)	−3	706 ± 138	∞	2.9 ± 0.8	151 ± 29
cGMP (5, 16[b])	−1	399 ± 35	548 ± 6.3	3.5 ± 1.8	163 ± 69
6-SH-cGMP (2)	−1	373 ± 112	275 ± 34	0.2	160
cIMP (1)	−1	436	780	0.3	83
cAMP (2)	−1	1292 ± 140	729 ± 110	4.4 ± 2.3	144 ± 45

[a] The charge is estimated at pH 7.4. The voltage dependence, expressed as mean ± SEM, was determined from an exponential fit to $K_{0.5}$ vs V (Hill) or K_b vs V (receptor effector). The parameters of the channel opening, K_o and V_0, are the median ± average deviation and were determined from the IV curve at saturation with eq 8. [b] Applies to $K_o(0)$ and V_0.

N_h, was 1.7 and voltage independent.

The voltage dependence of $K_{0.5}$ can be more clearly seen when the dose–response curves at each potential are normalized to the maximal current at saturating concentrations of cGMP. A family of scaled dose–response curves is plotted in the inset of Figure 4; the $K_{0.5}$ shifts to the left with increasing depolarization while the slope, N_h, remains constant.

All derivatives examined showed weak voltage dependence of $K_{0.5}$ that did not correlate with the net charge of the ligand species (Table II). The dissociation constant for most derivatives, including cGMP, varied e-fold over ~400 mV, but both Fl-cGMP and cAMP were significantly less voltage dependent than the other derivatives ($p < 0.05$). At present, we cannot reliably conclude that cAMP channel activation is less voltage dependent than Fl-cAMP activation due to the few cAMP curves which had sufficient data points for a reliable fit.

Discussion

Parameter Variability. The $K_{0.5}$ for cGMP in photoreceptors has previously been reported from 12 to 40 μM [for a review, see Pugh and Cobbs (1986)] with wide variability in the values. Similarly, the Hill coefficient has been reported from 1.6 to 3.4. We saw variability of ~20% (Table I) in the range of $K_{0.5}$ for all nucleotides. We also saw significant variations from the median in other parameters, particularly the change in IV rectification in Figure 2. We have been unable to attribute the variability to specific seasonal, biological, temporal, or experimental factors. Divalent cation effects arising from the choice of electrode glass (Furman & Tanaka, 1988) did not appear to be a factor in these experiments, and all saturation IV curves were well described by the simple open–close equilibrium model (see below). Other patch artifacts, such as loss of a soluble cytoplasmic factor, disruption of an attached cytoskeleton, or dephosphorylation (Rispoli et al., 1988), may underlie the large variance in our data and other patch studies.

Channel Reaction Schemes. At the present, information on the single channel properties of the nucleotide-activated channels or on the kinetics of the channel behavior (Haynes et al., 1986; Tanaka et al., 1987; Zimmerman & Baylor, 1986; Matthews & Watanabe, 1987, 1988) is too limited to impose many constraints on molecular models of the cGMP-activated channel reaction scheme. At low agonist concentrations, two conductance levels have been described (Haynes et al., 1986; Zimmerman & Baylor, 1986), but under physiological conditions, noise measurements have been interpreted as consistent with a single close–open reaction (Bodoia & Detwiler, 1984). Recently, channel data using "caged" cGMP under divalent-free conditions (Karpen et al., 1988) were well described by a single open state.

We have chosen two simple schemes to describe and interpret our data. (1) The classical Hill equation is a semiempirical scheme that assumes the receptors are completely bound or unbound by ligand, and in our case, the bound state is also the conducting state. The details of the reaction mechanism are ignored by treating only the input and output relations of the system. The equilibrium dissociation constant, $K_{0.5}$, is a measure of half-maximal saturation of the receptor sites with ligand, while the slope of the concentration–response curve at $K_{0.5}$, N_h, is interpreted as the mean square deviation of the number of ligands bound at half-saturation (Dahlquist, 1978) or as the minimum number of binding sites on the protein (Weber & Anderson, 1965). (2) To account explicitly for the voltage dependence of the IV curve, the Hill model can be extended by considering the cGMP-activated channel as a tightly coupled receptor–effector system where the fully ligand bound protein isomerizes to the conducting state. N_h has the previous meaning, but now there are two equilibrium dissociation constants describing the ligand binding and channel isomerization to the conducting state, respectively.

Voltage Dependence of Channel Gating. Our goals in modeling the voltage dependence of the IV curve are to determine if partial agonists, such as cAMP, exert their effect by altering the probability of channel opening and if the voltage dependence of channel gating explains the voltage dependence of binding, $K_{0.5}$, observed with the Hill equation (eq 1). To achieve these goals, we require an expression describing the steady-state, macroscopic current as a function of ligand concentration and transmembrane voltage.

The macroscopic current as a function of voltage for a mechanism with a single conducting state reflects the number of channels in a patch N, the single channel current (or, equivalently, the slope conductance g times the voltage V), and the voltage-dependent probability of channel opening $p(V)$:

$$I(V) = NgVp(V) \quad (2)$$

Since the single channel conductance, g, in symmetrical NaCl solutions is constant over the range −150 to +50 mV (Matthews & Watanabe, 1987) and, by assumption, the total number of channels in a patch, N, is constant, any nonlinearity in the IV response must result from voltage-dependent changes in the probability of channel gating.

The IV data at saturating nucleotide concentrations are well described by a simple voltage-dependent close–open equilibrium over the range −90 to +90 mV:

$$C \underset{k_{-1}}{\overset{k_1}{\rightleftharpoons}} O \quad (3)$$

Voltage dependence of this scheme is commonly attributed to the closing rate constant, $k_{-1}(V) = k_{-1}(0)e^{-V/V_0}$, where $k_{-1}(0)$ is the closing rate constant at zero potential, V is the potential across the membrane, and V_0 is the potential required for an e-fold change of rate. As we have steady-state, not kinetic, data, we define a dimensionless equilibrium constant:

$$K_o(V) = k_1/k_{-1}(V) = K_o(0)e^{-V/V_0} \quad (4)$$

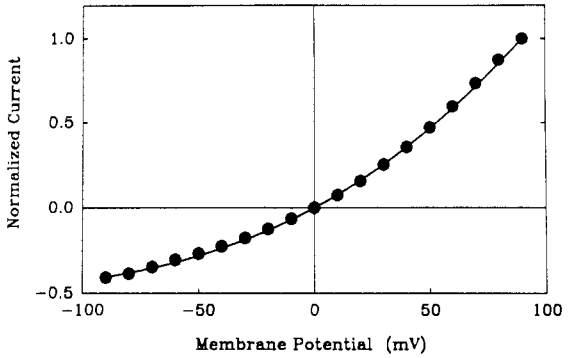

FIGURE 5: Voltage dependence of the channel gating at saturating concentrations of cGMP. The current activated at 200 μM cGMP from −90 to +90 mV (●) was scaled by the current at +90 mV. The solid line is the best fit of the voltage dependence of a close–open isomerization (eq 8). For this patch $K_o(0)$ was 3.3, V_0 was 151 mV, χ^2 was 6.7, and Q was 0.99 (patch 75263).

The steady-state probability of opening, $p(V)$, is equal to the sum of the observable states divided by the sum of all states in the reaction, or

$$p(V) = \frac{[O]}{[O] + [C]} \tag{5}$$

Substituting $K_o = [C]/[O]$ in eq 5 and simplifying gives the expression

$$p(V) = 1/[1 + K_o(V)] \tag{6}$$

Substituting eq 6 into eq 2 gives the steady-state macroscopic current as a function of voltage:

$$I(V) = \frac{NgV}{1 + K_o(0)e^{-V/V_0}} \tag{7}$$

The dependence of eq 7 on the number of channels, N, and the single channel conductance, g, can be removed by dividing eq 7 by $I(90)$, the current at +90 mV, giving

$$I(V) = \frac{[1 + K_o(90)]V}{[1 + K_o(V)]90} \tag{8}$$

This expression was fit to the normalized IV data at saturating ligand concentration with the Levenberg–Marquardt algorithm to obtain estimates for $K_o(0)$ and V_0.

Figure 5 shows the result of fitting eq 8 to the IV data of a cGMP-activated patch. The fits for all nucleotides on individual patches were statistically excellent ($Q > 0.95$), but the range of the fitted parameters was broad as previously discussed. This point can be appreciated by comparing the nearly linear IV curve at saturating cGMP in Figure 2B with the typical curved cGMP IV's shown in Figure 2A and Figure 5. Median values of $K_o(0)$ and V_0 for all ligands are summarized in Table II.

In general, no quantitative difference in the gating parameters, $K_o(0)$ and V_0, was noted among cGMP, Fl-cGMP, and cAMP which would explain the effects of partial agonists. The small values of $K_o(0)$ for 6-SH-cGMP and cIMP, however, probably reflect small sample bias as comparably small values were occasionally seen with cGMP.

The cross-correlation matrix computed for the estimated parameters, $K_o(0)$ and V_0, shows that they are strongly correlated ($r = 0.99$) and, therefore, not unique. Larger values for both parameters also provide statistically good fits, but as the parameters increase, the probability of channel opening asymptotically approaches zero. We, therefore, reported parameters that maximized the probability of channel opening. The probability of maximal channel opening computed with eq 6 is ~33%, consistent with recent measurements on cGMP-activated channels found on the inner segment (Matthews & Watanabe, 1988). In our analysis, we also assumed a constant single channel conductance, but if this assumption is incorrect, the model fit remains statistically valid. In such a case, physical interpretation of the model parameters as representing the probability of channel opening alone must be redefined to include an aspect of the free-energy profile an ion experiences in crossing through the channel.

Does Voltage-Dependent Gating Explain Voltage-Dependent Binding? The demonstration of a voltage-dependent shift in ligand concentration necessary for half-maximal response (Figure 4) might be explained by the voltage-dependent gating of the close–open isomerization, by voltage-dependent ligand binding, by intermediate voltage-dependent conformational changes, or by a combination of such factors. The simplest assumption is that the larger voltage dependence of channel opening, V_0, observed at saturating concentrations of cGMP (eq 8) accounts for all the voltage-dependent shift of $K_{0.5}$ determined from the Hill equation (eq 1). This assumption can be modeled by modifying the Hill equation to account for a tightly coupled binding step linked to an isomerization to the open conformation:

$$nL + C \overset{K_b}{\rightleftharpoons} L_nC \overset{K_0}{\rightleftharpoons} O \tag{9}$$

where K_b is the equilibrium constant for half-maximal saturation and K_o was defined previously (eq 4) for saturating ligand concentrations.

The steady-state probability of channel opening as a function of both voltage and ligand concentration can be obtained in an analogous manner to the derivation of eq 5. The fraction of channels in the open state at some voltage V is

$$p(V) = \frac{[O]}{[O] + [L_nC] + [C]} \tag{10}$$

Substituting $n = N_h$, the equilibrium constants $K_b^{N_h} = [L]^{N_h}[C]/[L_nC]$ and $K_o(V) = [L_nC]/[O]$, and $p(V) = I([L],V)/I_{max}([sat],V)$ into eq 10 and simplifying give

$$I([L],V) = \frac{I_{max}([sat],V)}{1 + K_o(V)[1 + (K_b/[L])^{N_h}]} \tag{11}$$

By using the individual estimates of $K_o(0)$ and V_0 previously obtained in each patch at saturation, eq 8, as fixed parameters, new estimates of the binding parameters, K_b and N_h, can be obtained by fitting the concentration–current data at each potential, V, with eq 11.

Both the goodness of fit, χ^2, and N_h are unchanged by fitting the data with eq 11 instead of eq 1 as expected, but the ligand concentration for half-saturation, K_b, increases between 11 and 80% compared with $K_{0.5}$ (Table I). In Fl-cGMP patches, the voltage dependence of gating accounted for all the voltage dependence of the overall reaction as hypothesized (see below and Figure 6B). For all other ligands, however, the voltage dependence of the binding dissociation constant, K_b, was only slightly reduced by the introduction of explicit voltage dependence in the channel opening step (Figure 6A and Table II).

The voltage dependence of channel gating, V_0, in reaction 3 or 9 is significantly steeper than the voltage dependence of $K_{0.5}$ observed with the Hill equation (eq 1) and Table II, but we would like to understand why voltage-dependent gating does not account for voltage-dependent binding.

The contribution of the voltage-dependent gating parameters, $K_o(0)$ and V_0, to the overall voltage dependence of $K_{0.5}$

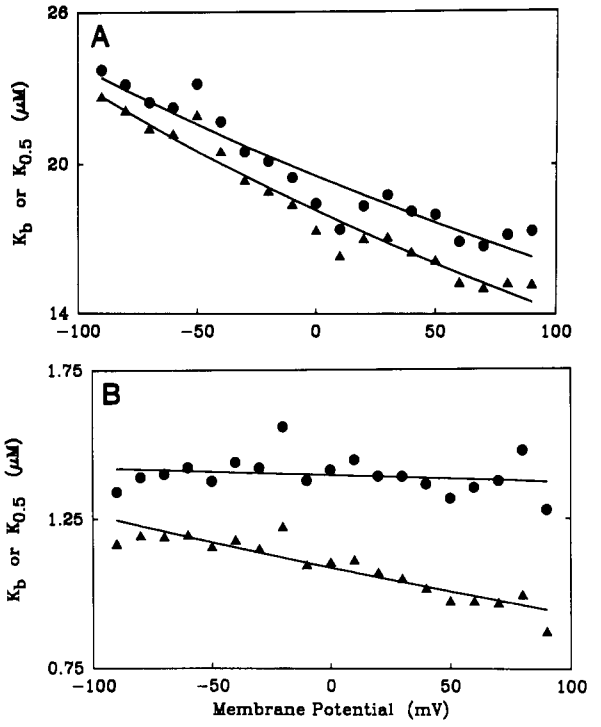

FIGURE 6: Voltage dependence of cGMP and Fl-cGMP dissociation constants. The $K_{0.5}$ values for cGMP (A) and Fl-cGMP (B) current activation (▲) and the voltage dependence of K_b (●) were obtained from fitting at each potential the Hill equation (eq 1) and the Hill receptor-effector equation (eq 11), respectively. Solid lines are the best exponential fits. While $K_{0.5}$ is less than K_b at all potentials, the voltage dependence of the Fl-cGMP dissociation constant (B), but not the cGMP dissociation constant (A), is not eliminated by accounting for the explicit voltage dependence of the nonlinearity of the IV relation (see Figure 2 and text). For the patch in (A) the voltage dependence of $K_{0.5}$ was −401, K_b was −494 mV/e-fold, $K_o(0)$ was 5.5, and V_0 was 180 mV (patch 75282). For (B) $K_{0.5}$ was −652, K_b was −5444 mV/e-fold, $K_o(0)$ was 1.74, and V_0 was 147 mV (patch 75261).

can be described analytically by substituting [L] = $K_{0.5}$ and $I/I_{max} = 0.5/(1 + K_o)$ into eq 11 and solving for $K_{0.5}$, giving

$$K_{0.5} = K_b[K_o(V)/[1 + K_o(V)]]^{1/N_h} \quad (12)$$

For $K_o(V) < 1$, eq 12 can be approximated by

$$K_{0.5} \simeq K_b K_o(V)^{1/N_h} \quad (13)$$

using an expansion series for the bracketed expression in eq 12. If K_b is voltage independent, then for small K_o the voltage dependence of the overall reaction is N_h times less than the voltage dependence of gating, V_0, as expected initially. For $K_o(V) > 1$, however, eq 12 can be approximated by

$$K_{0.5} \simeq K_b[1 - 1/K_o(V)]^{1/N_h} \quad (14)$$

As $K_o(V)$ becomes large, $K_{0.5}$ asymptotically approaches voltage independence.

Assuming K_b is voltage independent and using the average values of N_h and $K_o(V)$ for cGMP (Tables I and II), the expected voltage dependence of $K_{0.5}$ calculated with eq 14 is 1600 mV/e-fold compared to 400 mV/e-fold observed experimentally. K_b, however, may be voltage dependent as the activating nucleotides bear a net negative charge. The decrease in $K_{0.5}$ with depolarization, however, is opposite that expected for a negatively charged ligand approaching a binding site within the transmembrane electric field (Woodhull, 1973). We therefore conclude that the cyclic nucleotide binding sites lie outside the electric field on the cytoplasmic side of the protein and that the overall activation reaction has more voltage dependence than that conferred solely by channel gating.

The voltage dependence of the concentration–response curves is not explained completely by either voltage-dependent gating or voltage-dependent nucleotide binding in the hypothesized reaction mechanisms. The simplest explanation is to postulate the existence of an additional voltage-dependent isomerization before the observed conductance step:

$$nL + C \overset{K_b}{\rightleftharpoons} L_nC \overset{K_i(V)}{\rightleftharpoons} C' \overset{K_o(V)}{\rightleftharpoons} O \quad (15)$$

For Fl-cGMP, however, $K_i(V)$ is voltage independent perhaps because the greater charge (Table II) of the bound ligand attenuates the channel's dipole moment. The cooperativity of all ligand responses was insensitive to the transmembrane electric field. For the single effector states, this finding is expected, but alternative reaction schemes with multiple, parallel open states may lead to voltage-dependent cooperativity.

Comparison with Karpen et al. Model. The analysis of our equilibrium binding data shows both similarities and differences with the conclusions of Karpen et al. (1988) from kinetic measurements with the cGMP-activated channel. In each case the assumption that the binding of three ligands activates a single conducting state of the channel is sufficient to describe the current. The opening isomerization has approximately the same voltage dependence (our 163 mV vs their 123 mV), but their equilibrium dissociation constant for channel closing (0.006) is ~60 times smaller than our value (3.5). The most salient difference in both results is that the voltage dependence of channel gating of Karpen et al. completely accounts for the entire voltage dependence of activation, while, except for Fl-cGMP, gating explains only a small portion of the voltage dependence in our case. While smaller values for the dissociation constant theoretically confer more voltage sensitivity on reaction 9 with eq 13, the smaller values of Karpen et al. did not fit our data. In a few, individual cases where the actual value of our gating parameters were similar to those of Karpen, we still did not see a significant reduction in the voltage dependence of activation as predicted for reaction 9.

Conclusions

Our analysis of the voltage dependence of channel gating at saturating nucleotide concentrations showed that changes in the probability of channel opening could account for only a fraction of the effects of partial agonists and does not account for the voltage dependence of binding. We offer several possible explanations which can be explored in future studies. First and most obvious is that partial agonists may reduce the single channel conductance by a direct effect on the tertiary structure of the channel. Second, the transition to the open state may involve a series of closed but fully ligand bound states in which only the rate constants of the last close–open transition are independent of the species bound. A variation on this idea, consistent with the observation of several conductance states by Zimmerman and Baylor (1986) and Haynes et al. (1986), is that partial agonists may activate the lower conductance states preferentially.

These studies also provide evidence that the nucleotide binding sites lie outside the membrane electric field. We predict that the region of the channel involved in gating lies deeper in the protein as shown by the voltage dependence of the opening conformational change.

Our studies with cGMP derivatives have shown that substitutions at the 8-position affect only ligand binding but changes in C(2) and C(6) affect both binding and channel opening probability or single channel conductance. In contrast to certain other nucleotide binding proteins, the 3′,5′-diester

and the 2′-oxygen on the ribose are essential for binding.

ACKNOWLEDGMENTS

We thank Dr. David Jameson for many valuable discussions of this work, particularly regarding fluorescent derivatives; we also thank Dr. Sitaramayya Ari for his participation in initial experiments. We are grateful to the Center for Fluorescence Dynamics at the University of Illinois, Urbana, for the use of equipment and technical assistance on fluorescence polarization measurements.

Registry No. 8-Br-cGMP, 31356-94-2; 8-Fl-cGMP, 99776-42-8; 6-SH-cGMP, 57521-53-6; 2-amino-cPMP, 42467-66-3; cGMP, 7665-99-8; cIMP, 3545-76-4; cAMP, 60-92-4; GMP, 85-32-5; 2′-deoxy-cGMP, 13440-33-0; 8-SH-cGMP, 42154-49-4; 2-amino-PMP bicarbonate, 118890-22-5; 6-SH-GMP 4-morpholino-*N*,*N*-dicyclohexylcarboxamidium salt, 118868-33-0; 2-amino-PMP 4-morpholino-*N*,*N*-dicyclohexylcarboxamidium salt, 118868-34-1; thiourea, 62-56-6; 6-thioguanosine, 85-31-4; sodium, 7440-23-5.

REFERENCES

Adair, G. S. (1925) *J. Biol. Chem. 63*, 529.

Arai, K., Clark, B. F. C., Duffy, L., Jones, M. D., Kaziro, Y., Laursen, R. A., L'Italien, J., Miller, D. L., Nagarkatti, S., Nakamura, S., Nielson, L. M., Petersen, T. E., Takahashi, T., & Wade, M. (1980) *Proc. Natl. Acad. Sci. U.S.A. 77*, 1326–1330.

Bodoia, R. D., & Detwiler, P. B. (1984) *J. Physiol. (London) 367*, 183–216.

Caretta, A., Cavaggioni, A., & Sorbi, R. T. (1985) *Eur. J. Biochem. 153*, 49–53.

Catterall, W. A. (1988) *Science (Washington, D.C.) 242*, 50–61.

Cobbs, W. H., Barkdall, A. E., & Pugh, E. N., Jr. (1985) *Nature (London) 317*, 64–66.

Dahlquist, F. W. (1978) *Methods Enzymol. 48*, 270–299.

Ebright, R. A., LeGrice, F. J., Miller, J. P., & Krakow, J. S. (1985) *J. Mol. Biol. 182*, 91–107.

Eccleston, J. F. (1981) *Biochemistry 20*, 6265–6272.

Eccleston, J. F., Gratton, E., & Jameson, D. M. (1987) *Biochemistry 26*, 3902–3907.

Fesenko, E. E., Kaoesnikov, S. S., & Lyubarsky, A. L. (1985) *Nature (London) 313*, 310–313.

Fox, J. J., Wempen, I., Hampton, A., & Doerr, I. L. (1958) *J. Am. Chem. Soc. 80*, 1669–1675.

Furman, R. E., & Tanaka, J. C. (1988) *Biophys. J. 53*, 287–292.

Furman, R. E., & Tanaka, J. C. (1989) *Biochemistry* (following paper in this issue).

Haynes, L., & Yau, K.-W. (1985) *Nature (London) 317*, 61–64.

Haynes, L. W., Kay, A. R., & Yau, K.-W. (1986) *Nature (London) 321*, 66–70.

Hill, A. V. (1910) *J. Physiol. (London) 40*, 190.

Hille, B. (1984) *Ionic Channels of Excitable Membranes*, Sinauer Associates, Sunderland, MA.

Jurnak, F. (1985) *Science (Washington, D.C.) 230*, 32–36.

Karpen, J. W., Zimmerman, A. L., Stryer, L., & Baylor, D. A. (1988) *Proc. Natl. Acad. Sci. U.S.A. 85*, 1287–1291.

La Cour, T. F. M., Nyborg, J., Thirup, S., & Clark, B. F. C. (1985) *EMBO J. 4*, 2385–2388.

Lee, C.-H., & Sarma, R. H. (1976) *J. Am. Chem. Soc. 98*, 3541–3548.

Matthews, G., & Watanabe, S.-I. (1987) *J. Physiol. (London) 389*, 691–715.

Matthews, G., & Watanabe, S.-I. (1988) *J. Physiol. (London) 403*, 389.

Nakamura, T., & Gold, G. H. (1987) *Nature (London) 325*, 442–444.

Press, W. H., Flannery, B. P., Teukolsky, S. A., & Vetterling, W. T. (1986) *Numerical Recipes: The Art of Scientific Computing*, Cambridge University Press, Cambridge, U.K.

Pugh, E. N., Jr., & Cobbs, W. H. (1986) *Vision Res. 26*, 1613–1643.

Rispoli, G., Sather, W. A., & Detwiler, P. B. (1988) *Biophys. J. 53*, 388a.

Rossomando, E. F., Jahngen, J., & Eccleston, J. F. (1981) *Anal. Biochem. 116*, 80–88.

Smith, M., Drummond, G. I., & Khorana, H. G. (1961) *J. Am. Chem. Soc. 83*, 698–706.

Tanaka, J. C., Furman, R. E., Cobbs, W. H., & Mueller, P. (1987) *Proc. Natl. Acad. Sci. U.S.A. 84*, 724–728.

Tonosaki, K., & Funakoshi, M. (1988) *Nature (London) 331*, 354–356.

Weber, G., & Anderson, S. R. (1965) *Biochemistry 4*, 1942–1947.

Weber, I. T., Takio, K., Titani, K., & Steitz, T. A. (1982) *Proc. Natl. Acad. Sci. U.S.A. 79*, 7079–7083.

Weber, I. T., Steitz, T. A., Bubis, J., & Taylor, S. S. (1987) *Biochemistry 26*, 343–351.

Wittinghofer, A., Warren, W. F., & Leberman, R. (1977) *FEBS Lett. 75*, 241–243.

Woodhull, A. M. (1973) *J. Gen. Physiol. 61*, 687–708.

Yau, K.-W., Haynes, L. W., & Nakatani, K. (1986) *Fortschritte der Zoologie: Membrane Control*, Gustau Fischer Verlag, Stuttgart, FRG.

Zimmerman, A. L., & Baylor, D. A. (1986) *Nature (London) 321*, 70–73.

Zimmerman, A. L., Yamanaka, G., Eckstein, F., Baylor, D. A., & Stryer, L. (1985) *Proc. Natl. Acad. Sci. U.S.A. 82*, 8813–8817.